Title

Non common path aberration correction with non linear WFSs

Journal

Adaptive Optics for Extremely Large Telescopes 4 – Conference Proceedings, 1(1)

Authors

Esposito, Simone
Pinna, Enrico
Puglisi, Alfio
et al.

Publication Date

2015

DOI

10.20353/K3T4CP1131573

Non common path aberration correction with non linear WFSs

S. Esposito*[a], A. Puglisi[a], E. Pinna[a], G. Agapito[a], J.P. Veran[b], G. Herriot[b]
[a]Osservatorio Astrofisico di Arcetri, Largo E. Fermi 5, Firenze, Italy; [b]Herzberg Institute of Astrophysics, National Research Council of Canada, 5071 West Saanich Road, Victoria, British Columbia, Canada V9E 2E7

ABSTRACT

Non Common Path Aberrations (NCPA) are a usual problem encountered when using an Adaptive Optics System (AO) to produce corrected images in an astronomical instrument. The usual way to correct for such NCPA is to introduce an offset in the WaveFront Sensor (WFS) signals that corresponds to the aberration to correct. In such a way, when the AO loop is closed, the Deformable Mirror (DM) will converge to the shape required to null the NCPA. The method assumes that the WFS operation is linear and completely described by some pre-calibrated interaction matrix. This is not the case for some frequently used wavefront sensors like the Pyramid sensor or a quad-cell Shack-Hartmann sensor. Here we present a method to work in closed loop with a Pyramid Wavefront Sensor (PWS), or more generally a non linear WFS, while introducing a static offset on the DM. The DM shape is kept constant even if the AO residuals change over time because of variations of seeing, wind speed and so on. Results from numerical simulation and first on sky data from LBT FLAO system and LUCI2 facility instrument are presented.

Keywords: Non Common Path Aberration, Pyramid Sensor, Modal Control, Wavefront Sensing

1. INTRODUCTION

This work is an elaboration of previous studies done from several authors that considers the use of sinusoidal signal probes to calibrate different parameters of an AO system [1][2][3][4].
In the following work we will assume that the AO system is using a modal control approach where the wf is sensed and corrected in terms of a modal base of orthogonal modes. The block diagram of such an AO loop is represented in Figure 1.

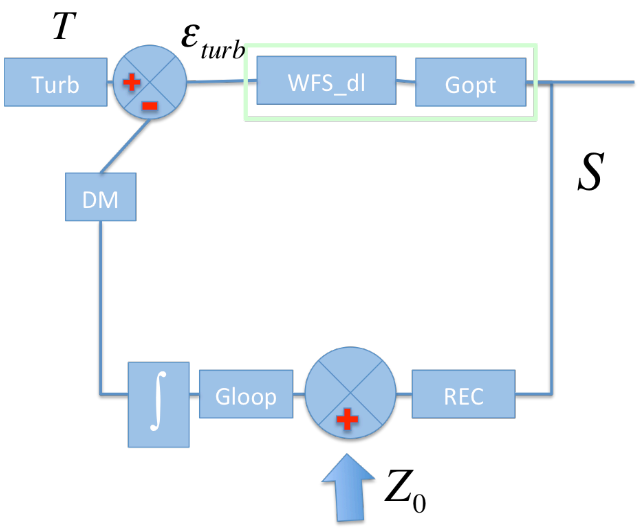

Figure 1. The block diagram reports the main elements of the loop. Note that the WFS block is made up of two parts. The second one is taking into account the WFS sensitivity change due to a change in the closed loop residuals. The term Z0 is added to include the NCPA.

where the WFS block is represented as the product of two different blocks. The two blocks allows dealing with a wavefront sensor where the output signal S depends on amount of aberrations of the input wavefront. The term Gopt is equal to one when the WFS is working with a Diffraction Limited (DL) PSF, and it is less than one when wavefront errors increase the size of the measured PSF. In particular, in the AO case, the term Gopt is changing depending on the efficiency of the correction. In the figure the term Z0 is a modal offset term that takes into account the considered NCPA. It is easy to show that in closed loop steady state the wavefront residual is given by

$$\varepsilon_{turb} = T\frac{G_{opt}}{G_{loop}} - \frac{Z_0}{G_{opt}} \tag{1}$$

The above equation shows that if Gopt=1 (the nominal condition) the NCPA is correctly applied but if Gopt<1 than the applied NCPA has a wrong amplitude.

2. OPTICAL GAIN CORRECTION

Here we present a method to measure the WFS optical gain Gopt and use this measurement to adjust the sensor behavior introducing the corrected NCPA value. We modify the loop block diagram as reported in Figure 2.

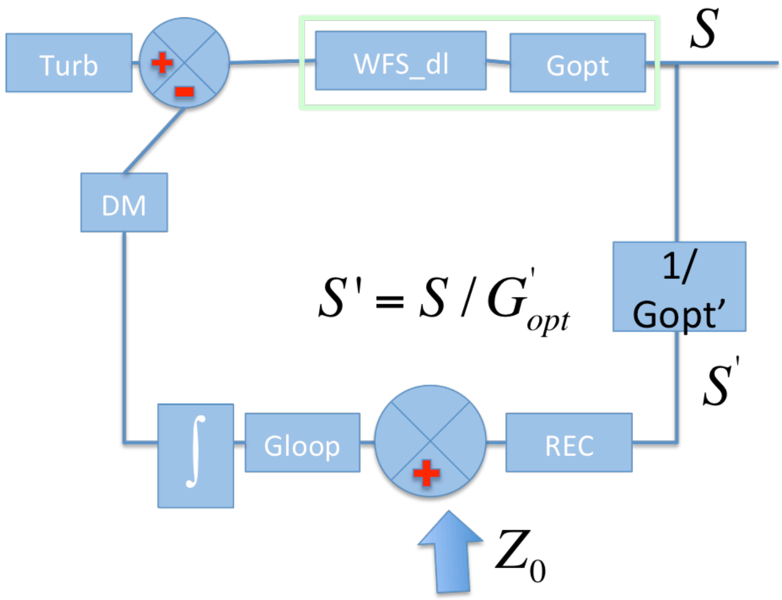

Figure 2. The diagram shows the normalization block introduced to take into account the Optical Gain changes. Here Gopt' is a measured value obtained from system telemetry as described below.

Here we added another block that multiply the sensor signal S by a factor 1/Gopt' and so doing renormalizes the achieved signals. It is easy to show that, as above, in closed loop now the wavefront residual E_{turb} is given by

$$\epsilon_{turb} = T^* \frac{G_{opt}}{(G'_{opt} G_{loop})} - Z_0 \frac{G'_{opt}}{G_{opt}} \tag{2}$$

Assuming that the input turbulence is 0 we find the closed loop residual that should be compensating the instrument NCPA. This is shown in eq.3

$$\epsilon_{turb} = -Z_0 \frac{G'_{opt}}{G_{opt}} \tag{3}$$

Here we see here that if the term Gopt'/Gopt = 1 than the NCPA value is correctly applied. To get such ratio equal to one we have to adjust the value of Gopt'.

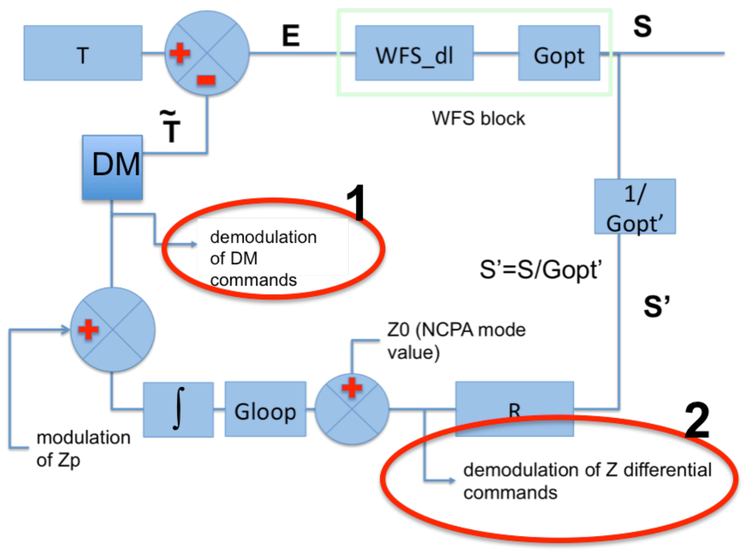

Figure 3. The complete block diagram describes the proposed methods. We highlighted the two demodulated signals we use to derive Gopt' and to run our Optical Gain tracking loop. Again NCPA term is represented as Z0 (bottom of the figure). The modulation signal is injected as Zp.

To such aim we introduce (using the AO DM) a sinusoidal signal at a frequency f and amplitude Zp. The modulation term is shown on the left of the figure. Following the figure above we define Zp_dem e Zp_dem_diff where the first is the modal signal demodulated from the DM commands (numbered 1 in the figure) and the second is the modal signal demodulated from differential commands at the output of the reconstructor (numbered 2 in the figure and taken before the multiplication for the loop gain Gloop). We note here that the demodulation of the DM commands is needed because the actual command originating from our modulation signal is affected by the control loop. With some computation we can show that:

$$\frac{Z_p^{dem}}{Z_p^{dif,dem}} = G_{opt}^{'} / G_{opt} \tag{4}$$

So, by using the demodulated signals discussed above we have a measurement of the critical ratio between Gopt' and Gopt. To provide the condition Gopt/Gopt' = 1 we introduce an integrator loop with error signal that:

$$\varepsilon = 1 - G_{opt}^{'} / G_{opt} \tag{5}$$

Gopt' is then updated at each tracking loop iteration using the formula that:

$$\left(G_{opt}^{'}\right)_k = (G_{opt}^{'})_{k-1} - G_{track}\varepsilon \tag{6}$$

The k index here identifies the various iterations of the tracking loop having a loop rate slower than the adaptive main loop.

3. NUMERICAL SIMULATION OF THE METHOD

We report here below some results achieved by numerical simulations. The simulated system is the AO NGS loop of the TMT telescope where we considered the NGS WFS to be a pyramid sensor. The turbulence main conditions are r0=18.6cm, L0=30m @0.5um (median seeing conditions at Mauna Kea). In order to test the NCPA correction we introduced a NCPA value of 150nm rms of astigmatism and 70nm wavefront rms of polishing error spatially distributed with a power law f^-2. The AO loop is going at a frame rate of 800 Hz while the sinusoidal modulation frequency is 80 Hz. The modulation signal is applied to the other astigmatism with amplitude of 9nm rms. As a first test we apply the NCPA without using the optical gain tracking loop and study the AO system temporal behavior.

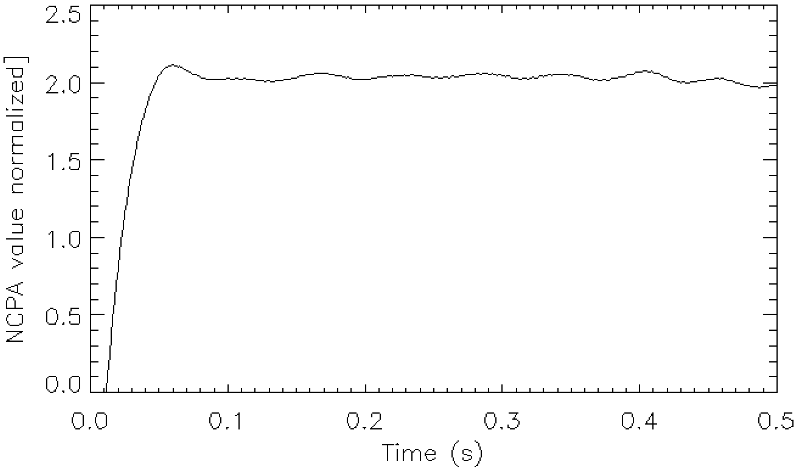

Figure 4. The temporal evolution of the NCPA correction in normalized units without applying the Optical Gain tracking loop. The picture shows that the system converges to an NCPA value twice the corrected one.

From Figure 4 where the amount of NCPA applied is shown we see that the system converge to an NCPA value twice the good one. The simulations confirm the results we showed above stating that the system will converge to the NCPA value multiplied by the ration Gopt/Gopt'. In particular because the system is calibrated in DL conditions the mentioned ratio is smaller than one leading to an overestimate of the applied NCPA. The same time evolution is shown in fig. 5 when the Optical Gain tracking loop is active.

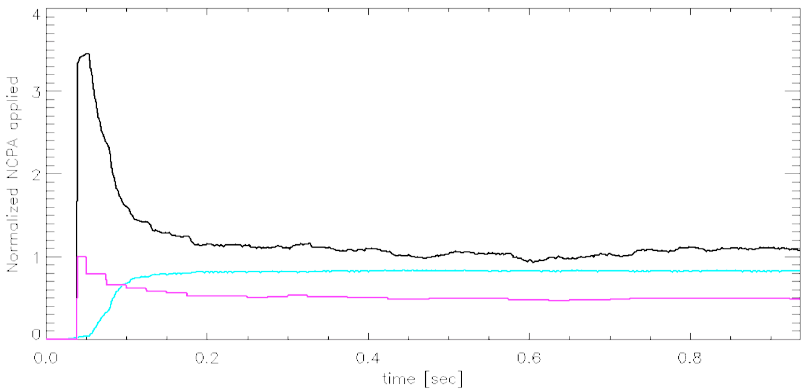

Figure 5. Same as above but with the tracking loop on. NCPA is properly corrected and the Optical Gain is estimated to be about 0.5, consistently with the applied aberration found before being twice the required value.

We see in Figure 5 that the NCPA applied value is increasing initially but is then converging to the correct normalized value of 1 (black curve). At the same time the achieved SR in H band is 82% (light blue curve) and the actual optical gain Gopt is estimated to be 0.5 (pink curve). This number is consistent with previous results where applied NCPA value without optical gain tracking loop was twice the nominal one. Simulations clearly show that the considered approach for optical gain tracking of a pyramid sensor is working. The required modulation signal has a wavefront rms of 9nm. But as mentioned already above the effective signal amplitude is reduced by the loop and is actually about 5nm. This small wavefront error is mostly negligible for the instrument error budget. We note here that the methods required a good knowledge of the mirror commands, for example hysteresis effects are not considered in our simulations. We note in passing that the measurement of the Optical Gain tracking loop allows to keep the AO system overall gain constant while seeing and correction efficiency is changing.

4. TEST WITH LUCI2 AT THE LBT TELESCOPE

We tested the method described above at the LBT telescope using the FLAO system [5][6] and the LBT infrared imager and multi-object spectrograph LUCI2 [7][8]. An initial test has been done in daytime using our calibration fiber that allows running the FLAO system in closed loop generating the atmospheric disturbances directly with the adaptive secondary mirror. The main parameters settings for the technique are reported in Table 1.

Table 1. Main parameters for the Optical Gain tracking loop.

Sinusoidal signal amplitude	Sinusoidal signal frequency	Track loop iteration rate	Injected mode	Acquisition time for tracking loop
10nm	30 Hz	0.25 Hz (4s)	KL 4 (astig.)	4s

The NCPA of LUCI2 has been first measured and then the corresponding Zernike coefficients has been decomposed on our Karhunen-Loeve (KL) modal base and applied as offset in the differential commands calculated by the system RTC. The PSF of LUCI2 has been acquired without and with the NCPA correction applied. The results are shown in Figure 6.

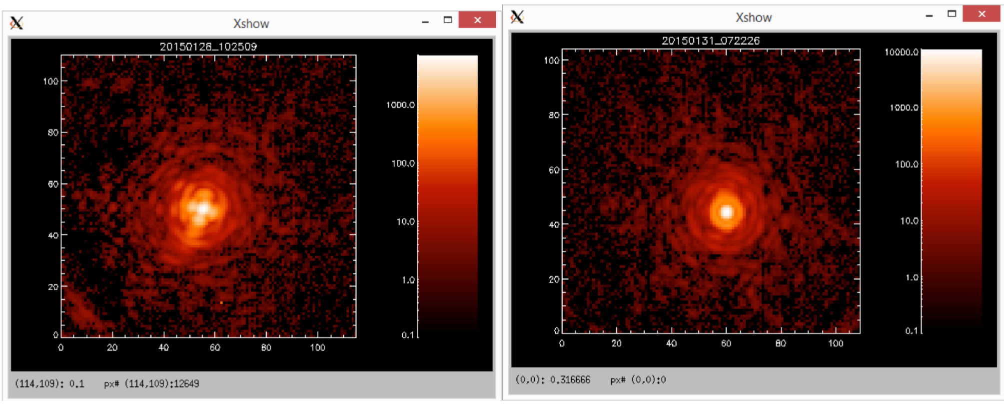

Figure 6. Example of two LUCI PSF without and with NCPA applied during daytime test.

The image on the left side shows the PSF before NCPA introduction while image on right is after NCPA introduction. The achieved H band SR in the two images is respectively 0.35 and 0.7 for uncorrected and corrected. The same results are achieved when an atmospheric disturbance is applied using the adaptive secondary as mentioned above. This is shown in Figure 7 where even with a 1.5 arcsecond seeing of introduced disturbance the PSF profile remain stable up to 200 mas of distance from the center showing that the correction of astigmatism provided by the methods is not degraded significantly by the seeing. In other words the loop is able to apply a stable wavefront offsets even if the efficiency of the correction is changing. As a final result we report some images taken on sky with injected NCPA and the optical gain tracking loop on.

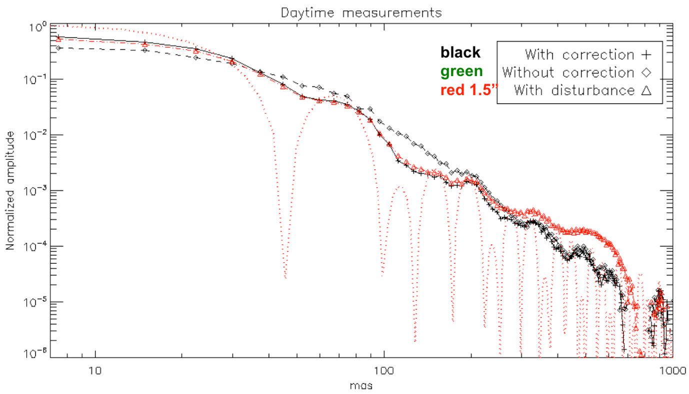

Figure 7. The different averaged azimuthal profiles of the PSF in the three cases, without NCPA, with NCPA and with NCPA and atmospheric disturbance.

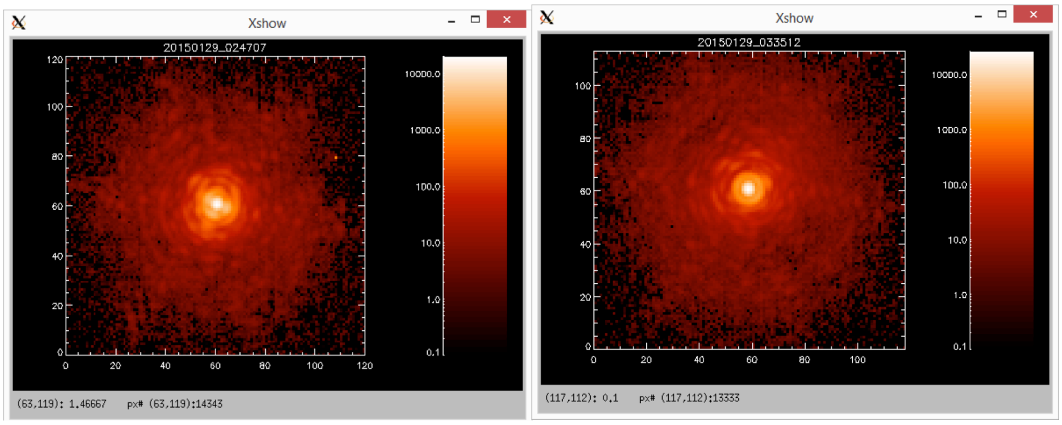

Figure 8. Example of two LUCI PSF without and with NCPA applied measured during on-sky test.

Again in Figure 8 the left side PSF is achieved without NCPA injection while the right side is with the NCPA injection and tracking loop on. The H band SRs of the images is 0.37 and 0.7 respectively.

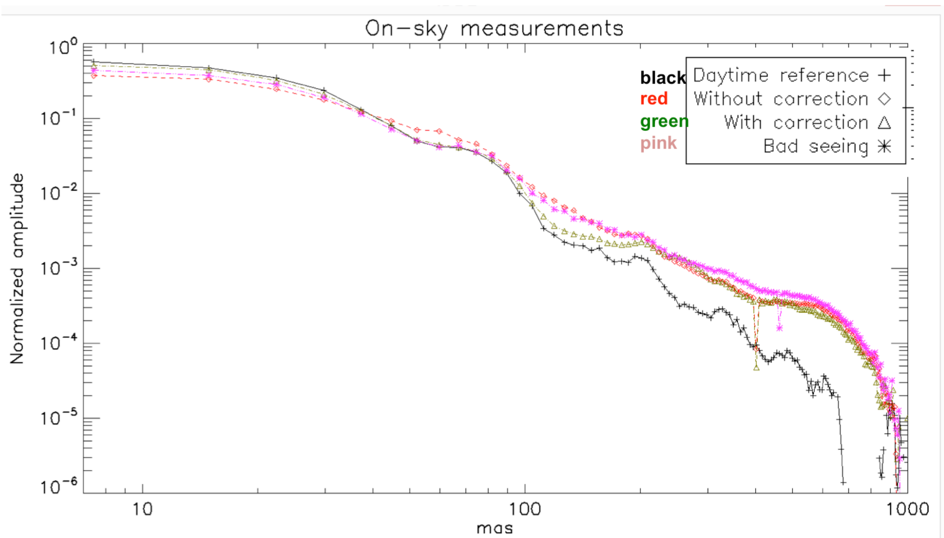

Figure 9. On sky averaged azimuthal profiles for the example PSFs showed above.

In terms of stability of the correction as a function of seeing we report the PSF profiles in Figure 9 for different seeing conditions to show as above that the PSF remains stable where the effect of the astigmatism correction is higher namely up to the first ring.

5. CONCLUSIONS

We presented a new method to work with non linear wavefront sensors like pyramid wavefront sensors. The method can be quite important in the typical case where such sensors are required to apply non common path aberration by using offsets in the sensor signals. The use of a sinusoidal reference signal injected in the system allows measuring the actual system gain and enables to apply the proper NCPA value. Numerical simulations done for the case of the TMT telescope with standard turbulence conditions has been done using a small 9nm rms sinusoidal signal that allows to control the system. In particular, with the tracking loop on, an NCPA of 165nm of NCPA is corrected to a residual of 6nm rms. First results in daytime and on sky at the LBT telescope show that the technique improves the images SR from 0.35 to 0.7 and provide stable PSF static correction against the seeing variation.

REFERENCES

[1] Esposito, S. and Tubbs, R. and Puglisi, A. and Oberti, S. and Tozzi, A. and Xompero, M. and Zanotti, D., "High SNR measurement of interaction matrix on-sky and in lab", in *Advances in Adaptive Optics II*, proc. SPIE 6272, 2006.

[2] Oberti, S. and Quirós-Pacheco, Fernando and Esposito, S. and Muradore, R. and Arsenault, R. and Fedrigo, E. and Kasper, M. and Kolb, J. and Marchetti, E. and Riccardi, A. and Soenke, C. and Stroebele, S." Large DM AO systems: synthetic IM or calibration on sky?", in *Advances in Adaptive Optics II*, proc. SPIE 6272, 2006.

[3] Véran, Jean-Pierre and Herriot, Glen, "Centroid gain compensation in Shack-Hartmann adaptive optics systems with natural or laser guide star", J. Opt. Soc. Am. A 17(8), pp. 1430-1439, August 2000.

[4] Saddlemyer, Leslie K. and Herriot, Glen and Véran, Jean-Pierre and Smith, Malcolm and Dunn, Jennifer, "Innovations within the Altair real-time wavefront reconstructor", in *Advancements in Adaptive Optics*, proc. SPIE 5490, 2004.

[5] Esposito, S. and Riccardi, A. and Pinna, E. and Puglisi, A. and Quirós-Pacheco, F. and Arcidiacono, C. and Xompero, M. and Briguglio, R. and Agapito, G. and Busoni, L. and Fini, L. and Argomedo, J. and Gherardi, A. and Brusa, G. and Miller, D. and Guerra, J.C. and Stefanini, P. and Salinari, P., "Large Binocular Telescope Adaptive Optics System: new achievements and perspectives in adaptive optics", in *Astronomical Adaptive Optics Systems and Applications IV*, proc. SPIE 8149, 2011.

[6] Esposito, S. and Riccardi, A. and Fini, L. and Puglisi, A.T. and Pinna, E. and Xompero, M. and Briguglio, R. and Quirós-Pacheco, F. and Stefanini, P. and Guerra, J.C. and Busoni, L. and Tozzi, A. and Pieralli, F. and Agapito, G. and Brusa-Zappellini, G. and Demers, R. and Brynnel, J. and Arcidiacono, C. and Salinari, P., "First light AO (FLAO) system for LBT: final integration, acceptance test in Europe, and preliminary on-sky commissioning results", in *Adaptive Optics Systems II*, proc. SPIE 7736, 2010.

[7] Seifert, W. and Ageorges, N. and Lehmitz, M. and Buschkamp, P. and Knierim, V. and Polsterer, K. and Germeroth, A. and Pasquali, A. and Naranjo, V. and Jütte, M. and Feiz, C. and Gemperlein, H. and Hofmann, R. and Laun, W. and Lederer, R. and Lenzen, R. and Mall, U. and Mandel, H. and Müller, P. and Quirrenbach, A. and Schäffner, L. and Storz, C. and Weiser, P., "LUCIFER1: performance results", in *Ground-based and Airborne Instrumentation for Astronomy III*, proc. SPIE 7735, 2010.

[8] Buschkamp, P. and Seifert, W. and Polsterer, K. and Hofmann, R. and Gemperlein, H. and Lederer, R. and Lehmitz, M. and Naranjo, V. and Ageorges, N. and Kurk, J. and Eisenhauer, F. and Rabien, S. and {Honsberg}, M. and Genzel, R., "LUCI in the sky: performance and lessons learned in the first two years of near-infrared multi-object spectroscopy at the LBT", in *Ground-based and Airborne Instrumentation for Astronomy IV*, proc. SPIE 8446, 2010.